

Effects of interaction on the properties of spiral galaxies

II. Isolated galaxies: The zero point*

I. Márquez¹ and M. Moles^{2,3,**}

¹ Instituto de Astrofísica de Andalucía (C.S.I.C.), Apdo. 3004, E-18080 Granada, Spain

² Instituto de Matemáticas y Física Fundamental (C.S.I.C.), C/Serrano 123, E-28006 Madrid, Spain

³ Observatorio Astronómico Nacional, Madrid, Spain

Received 9 November 1998 / Accepted 18 January 1999

Abstract. We analyse the properties of a sample of 22 bright isolated spiral galaxies on the basis of Johnson B,V,I images and optical rotation curves. The fraction of early morphological types in our sample of isolated galaxies (or in other samples of non-interacting spiral galaxies) appears to be smaller than in samples including interacting systems. The overall morphological aspect is regular and symmetric, but all the galaxies present non-axisymmetric components in the form of bars or rings. We find that the color indices become bluer towards the outer parts and that their central values are well correlated with the total colors. The properties of the bulges span a larger range than those of the disks, that thus are more alike between them. None of the galaxies shows a truncated, type II disk profile. It is found that the relation between surface brightness and size for the bulges, the Kormendy relation, is tighter when only isolated galaxies are considered. We find a similar relation for the disk parameters with an unprecedented low scatter.

A Principal Component Analysis of the measured parameters shows that 2 *eigenvectors* suffice to explain more than 95 % of the total variance. These are, as found for other samples including spiral galaxies in different environmental situations, a scale parameter given by the mass or, equivalently, the luminosity or the size; and a form parameter given by the bulge to disk luminosity ratio, B/D, or, equivalently, by the gradient of the solid-body rotation region of the rotation curve, the G-parameter. We report here a tight correlation between G and B/D for our sample of isolated spirals that could be used as a new distance indicator.

Key words: galaxies: fundamental parameters – galaxies: interactions – galaxies: kinematics and dynamics – galaxies: photometry – galaxies: spiral – galaxies: structure

1. Introduction

It is generally admitted that gravitational interaction can modify the properties of galaxies in rich environments. Its effects are often invoked to explain different observed properties, from the distribution of morphological types in clusters of galaxies to the peculiarities sometimes seen in particular galaxies. Those effects, on the other hand, can be very diverse in nature and have very different time scales to manifest, so it is not straightforward to ascertain whether such or such peculiarity is actually the fact of the interaction. In other words, the absence of peculiarities in a given system cannot be given as a sign of isolation, whereas the presence of unusual features cannot be unambiguously given as a proof of gravitational interaction (see Moles et al. 1994, for the pair NGC 450/UGC 807).

It is clear that the characterization of the specific effects of the gravitational interaction needs to be preceded by the exhaustive analysis of the properties of galaxies that could be considered as isolated. The average values and the ranges they present in size, luminosity, bulge to disk ratio, etc, do constitute the starting point to which refer similar properties of spirals in richer environments, from isolated pairs and small groups to clusters. Only such a comparative analysis could eventually lead to the identification of the specific effects of the gravitational interaction. This interaction is expected to produce changes in some morphological aspects, the kinematics, and the stellar content of the involved galaxies. Thus, it is necessary to start with the study of those same properties for a well defined sample of isolated galaxies.

Important studies of samples of spiral galaxies do exist, but these, even if sometimes defined as containing normal or non-peculiar galaxies, include galaxies belonging to interacting systems. The first important contribution to the study of galactic kinematics was made by Rubin and collaborators (Rubin et al. 1991, and references therein). A total of about 60 galaxies, se-

Send offprint requests to: I. Márquez (isabel@iaa.es)

* Based on data obtained at the 1.5m telescope of the Estación de Observación de Calar Alto, Instituto Geográfico Nacional, which is jointly operated by the Instituto Geográfico Nacional and the Consejo Superior de Investigaciones Científicas through the Instituto de Astrofísica de Andalucía

** Visiting Astronomer, German-Spanish Astronomical Center, Calar Alto, operated by the Max-Planck-Institut für Astronomie jointly with the Spanish National Commission for Astronomy

lected to cover a wide range in size, mass, and luminosity were observed. There was no aim to build up a complete sample, and most of the objects are non isolated. Moreover, the ulterior photometric analysis (Kent 1988, and references therein) has been done only for some of them, so complete data are only available for a relatively small number of field spirals. Further studies have considerably increased the number of objects, but none of them took into account the information on the environmental status of the galaxies, and were focused either on the photometric properties (de Jong & van der Kruit 1994; de Jong 1996a, b, c; see Table 1 from Héreaudeau & Simien 1996; Peletier & Balcells 1997; more recently, Baggett et al. 1998 for one photometric band data) or to spectroscopic and imaging surveys of field galaxies for which the existing information is long slit spectra together with just one broad band (Mathewson et al. 1992; Courteau 1996).

It is not a simple question to define what an isolated galaxy is. We only try here to establish operational criteria to identify isolated systems. The perturbations that a galaxy can suffer depend, apart the properties of the galaxy itself, on the mass, size, distance and relative velocity of the perturbing agent. Thus, the influence of very far away big galaxies will be negligible, but small galaxies can produce secular alterations on the dynamics of the primary system provided they are close enough (Athanasoulas 1984; Sundelius et al. 1987; Byrd & Howard 1992). And they can manifest themselves on very different time scales. Here we define an isolated galaxy as that for which the possible past perturbations by neighboring galaxies, if any, have been completely erased by now. Accepting that typical time scales for the decay of the perturbation effects are not longer than a few times 10^9 years, a criterion for isolation can be given. As discussed in Márquez & Moles (1996; hereafter paper I), we consider a galaxy isolated when it has no neighbours in a volume defined by a radius of 0.5 Mpc in projected distance and a redshift difference of 500 km s^{-1} . To be conservative, we also discarded all those galaxies which appear on the POSS prints with close neighbours for which there is no redshift information (see below).

The present work, the second of three, is devoted to the study of the properties of a sample of isolated spiral galaxies. The case of spirals in isolated pairs will be presented in Paper III, whereas the description of both samples, the details of the observations, data reduction and methods of analysis were given in Paper I. We have both, CCD multi-color (Johnson B, V and I bands) photometry and major axis long slit spectra information, for 15 isolated spiral galaxies. For some of those galaxies we also present minor axis long slit spectra and/or $H\alpha$ CCD photometry. We also present long slit spectra for 4 more galaxies. The properties we have measured are compared with those of other analyses to find whether they are different. This contribution is organized as follows: The sample is briefly described in Sect. 2. In Sect. 3 we comment the morphological aspects. In Sect. 4 we analyse the set of parameters obtained from the whole data and in Sect. 5, the relationships among them. The conclusions are presented in Sect. 6.

2. The sample of isolated galaxies

In configuring our sample of isolated spiral galaxies, the first step was to select all the spirals brighter than $m_B = 13$ mag with $\delta > 0$ in the CfA catalogue (Huchra et al. 1983). For practical reasons only galaxies with diameters smaller than $4'$ were retained. To minimize inclination corrections for both photometric and kinematical data, we only considered objects with inclinations between 32° and 73° (i.e., catalogued b/a in the range $0.8 < b/a < 0.3$). The sample selected in that way is magnitude and size limited.

After that we defined a criterion for isolation. We first excluded all the galaxies that are in the catalogues by Karachentsev (1972), Turner (1976) or Soares (1989), that is to say, well characterized members of isolated pairs or small groups. Then, a galaxy was considered **isolated** when the nearest neighbor found in the CfA catalogue was outside the volume defined by a projected distance of 0.5 Mpc (we adopt here $H_0 = 75 \text{ km s}^{-1} \text{ Mpc}^{-1}$) and a redshift difference of 500 km s^{-1} . To eliminate the possibility of having small companions fainter than the limit of the CfA catalogue, that could be still very efficient in producing dynamical or morphological perturbations in the main galaxy (see quoted references and Márquez et al. 1996), we also excluded galaxies with optical companions in the Palomar Sky Survey Prints. The final sample contains 22 galaxies defined as isolated (see Table 1 in Paper I). It is found that all of them have $cz < 6000 \text{ km s}^{-1}$.

3. The morphology of the isolated galaxies

The RC3 catalogue (de Vaucouleurs et al. 1991) contains detailed morphological information for many of the 22 galaxies in our sample. There is information on the subtype for all the galaxies, with the exception of NGC 6155, classified just as spiral. There is catalogue information on the presence or not of a bar for 16 galaxies, and we were able to add that information for other 5 galaxies (UGC 3511, UGC 3804, NGC 3835, NGC 6155 and NGC 6395, see notes on individual galaxies in Paper I¹), so the bar information does exist for all the 22 galaxies but one, namely NGC 4525, classified as Scd. The morphological information is completed with details on the presence of rings for 17 galaxies in the sample.

Looking at that information, the following picture emerges. First, only 5 out of the 21 galaxies with type information are earlier than Sc. This could be just an artifact due to the limited size of our sample, but we note that de Jong & van der Kruit (1994) find also a type distribution that peaks at Sc for their sample of 86 non-interacting, non-peculiar spirals.

Among the 21 galaxies with information on the presence of a bar, 8 are non barred (SA), 3 are barred (SB) and 10 are weakly barred (type SAB coded as SX in the RC3). The fraction of barred systems among the isolated galaxies amounts to 62%. In spite of the small size of our sample, we notice that this fraction is very similar to that found for a large population of spirals,

¹ Published only in electronic form and available on the server of the Editions de Physique: <http://www.ed-phys.fr>

without consideration of their environmental status (Moles et al. 1995).

Another interesting aspect is that all the non-barred (SA) galaxies in the sample are ringed spirals. Therefore, all the 21 galaxies with bar or ring information do show the presence of features indicative of the presence of non-axisymmetric components of the potential. Indeed, this kind of structures is easily explained as due to perturbations of the gravitational potential by companions (Simkim et al. 1980; Arsenault 1989; Elmegreen et al. 1990; Combes & Elmegreen 1993). But the selection criteria we have adopted to define the sample of isolated spirals was designed to select objects that wouldn't have experienced gravitational interaction in the last 10^9 years at least. The presence of those components in all of them should imply longer time scales for those features, unless the possibility of spontaneous formation of such structures along the galactic life is accepted.

The global aspect of those galaxies is however quite regular. For the 17 galaxies for which we could gather CCD broad band images, our analysis shows that all their disks are quite symmetric at their outskirts. We have calculated the decentering degree as the displacement of the center of the most external, recorded isophote with respect to the luminosity center, normalized to the last measured radius. The values we measured are always smaller than 5%, except for NGC 6155, for which we found 10%. The average decentering amounts to $2.4 \pm 2.7\%$. Concerning the spiral arm structure, it can be generally described as regular and symmetric in shape, although sometimes it is more intense in one of the hemispheres. Essentially all kind of structuring are encountered in our isolated spirals but, we cannot extract statistically significant results on their arm structure due to the limited number of systems we have in the sample.

4. The photometric and kinematical properties

In Paper I we give the whole set of parameters measured for the sample of isolated galaxies, together with the descriptions of how they have been obtained. In Table 1 we show the median values together with the dispersion and the range of variation for the different measured parameters. Indeed, given the size of the sample it is not possible to give the values for each morphological subtype. Moreover, as we have discussed, most of the galaxies are late types, with 11 of them classified as Sc. We note that this aspect should act as a caution when trying to do comparative studies.

4.1. The photometric properties

4.1.1. Luminosity and color indices

The distances used to evaluate the luminosity were derived from the measured redshift corrected for galactocentric motion (as indicated in the RC2 catalogue, de Vaucouleurs et al., 1976), with $H_0 = 75 \text{ km s}^{-1} \text{ Mpc}^{-1}$. The correction for the Virgocentric inflow for our galaxies is in general small (always less than 15%) and, as discussed in Paper I, not sensitive to the detailed model used. We therefore decided not to correct for the inflow. The magnitudes and color indices given in Table 2 are corrected

Table 1. Average properties of the 22 isolated spirals in the sample.

| | | | |
|-----------------------|------------------|---------------------------|-------------------|
| t | 5 ± 1.4 | $-M_B^D$ | 19.98 ± 0.53 |
| $-M_B^0$ | 20.35 ± 0.54 | $-M_I^D$ | 21.70 ± 0.68 |
| $-M_V^0$ | 20.74 ± 0.60 | $-M_B^B$ | 17.80 ± 0.80 |
| $-M_I^0$ | 21.88 ± 0.85 | $-M_I^B$ | 20.44 ± 0.93 |
| $(B - V)_T$ | 0.48 ± 0.09 | $(B - I)_D$ | 1.75 ± 0.24 |
| $(B - I)_T$ | 1.67 ± 0.25 | $(B - I)_B$ | 2.52 ± 0.59 |
| $\langle \mu \rangle$ | 21.57 ± 0.28 | $(B - V)_c$ | 0.89 ± 0.10 |
| R_B^e | 4.3 ± 1.4 | $(B - I)_c$ | 2.21 ± 0.29 |
| R_V^e | 3.5 ± 1.2 | $-P_{(BV)}$ | 0.047 ± 0.019 |
| R_I^e | 3.2 ± 1.0 | $-P_{(BI)}$ | 0.077 ± 0.033 |
| D | 35 ± 12 | G | 157 ± 103 |
| i | 53 ± 10 | R_{max} (Kpc) | 4.00 ± 1.28 |
| a | 24.4 ± 9.6 | V_{max}^i | 179 ± 35 |
| b | 12.7 ± 6.7 | R_M (Kpc) | 8.0 ± 2.6 |
| $\mu_{B,D}^e$ | 22.61 ± 0.44 | V_M^i | 183 ± 35 |
| $R_{B,D}^e$ | 5.1 ± 1.5 | $Mass(R_M)$ | 7.5 ± 3.9 |
| $\mu_{B,B}^e$ | 20.10 ± 2.25 | $Mass(R_{25})$ | 10.3 ± 6.1 |
| $R_{B,B}^e$ | 0.22 ± 0.65 | V_{sist} | 2569 ± 859 |
| $\mu_{I,D}^e$ | 20.40 ± 0.54 | M/L_B | 4.1 ± 1.4 |
| $R_{I,D}^e$ | 3.6 ± 1.1 | $\Delta^{(1)}$ | 7.6 ± 7.1 |
| $\mu_{I,B}^e$ | 17.96 ± 2.35 | $\log(L_{H\alpha}^{(2)})$ | 41.2 ± 0.5 |
| $R_{I,B}^e$ | 0.73 ± 1.02 | | |
| $0.5 \times D_{25}^B$ | 10.01 ± 2.85 | | |
| $0.5 \times D_{25}^I$ | 12.93 ± 3.52 | | |

M are absolute magnitudes. All the R (effective radius) together with a and b (major and minor axes) are in Kpc. D are distances in Mpc ($H_0 = 75 \text{ km s}^{-1} \text{ Mpc}^{-1}$). $i = \arccos(b/a)$, in degrees. $\mu_{i,j}^e$ are surface brightness parameters in $\text{mag}/('')^2$, and $R_{i,j}^e$ the effective radii in Kpc, from the photometric decomposition, where i is the filter and j is the component (D =disk, B =bulge). O and P are the origin and slope of the linear regime of the color gradients (see text). G is in units of $\text{km s}^{-1} \text{ Kpc}^{-1}$. M/L_B is in solar units. Velocities are in km s^{-1} . Mass in $10^{10} M_\odot$ units

(¹) See text for the definition of $\Delta = \Delta V / \Delta R$ ($^\circ$)

(²) Luminosity in $10^{41} \text{ erg s}^{-1}$ units.

for galactic and internal extinction as explained in Paper I (see Table 7 in Paper I).

The range of the B luminosity of the galaxies we have measured is $-18.58 \leq M_B \leq -22.19$, with a median value of -20.35 (see Table 1). Therefore, there are no faint spirals in our sample, a fact that has to be taken into account when making comparative analysis (see below). The effective radii in Table 1 have been calculated from the growing curves in the different bands. The mean surface brightness values were evaluated for the area enclosed by the $25 \text{ mag}/('')^2$ isophote (taken from the RC3), i. e., $\langle \mu \rangle = -2.5 \log(I/r_{25}^2)$, where r_{25} is the radius of that isophote.

For the total color indices the ranges we find are $0.35 \leq (B - V) \leq 0.85$ and $1.2 \leq (B - I) \leq 2.4$. These are similar to what is found for other samples of spiral galaxies, independently of their interaction status (Roberts & Haynes 1994; de Jong 1996c).

To characterize the populations of the disks we have considered the color indices and their gradients along the disk. To

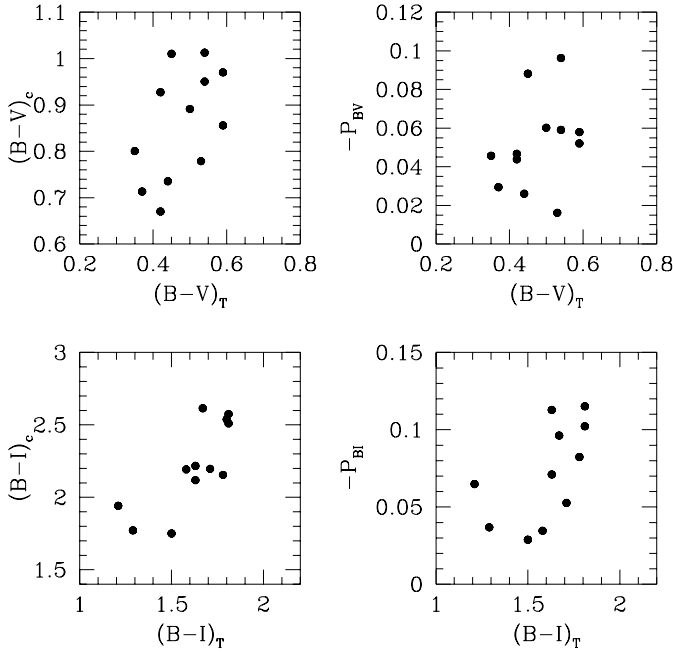


Fig. 1. The central colors, and the slope P of the color gradient (in magnitudes per kpc) as a function of the total galactic colors.

quantify the color gradients we have fitted a linear function of the form $CI(r) = CI(c) + Pr$, where $CI(c)$ is the (extrapolated) central color index under consideration, and r the radial distance in kpc. We find that P is negative for all the galaxies in the sample, i.e., their color indices become bluer towards the external parts. As shown in Fig. 1, the central color indices correlate with the corresponding total colors: they are redder for redder galaxies. The correlation is better traced by $(B - I)$, with correlation coefficient $r = 0.774$ and probability $P = 0.9969$. Another interesting aspect is that the central colors seem to span a wider range than outer colors, specially in $(B - I)$. We find $0.67 \leq (B - V)_c \leq 1.01$ and $1.75 \leq (B - I)_c \leq 2.61$ for the central colors, whereas for the colors measured at the last recorded isophote, R_B , we have $0.50 \leq (B - V) \leq 0.78$ and $1.52 \leq (B - I) \leq 2.17$ (UGC 3511 was excluded for this calculation since the colors we measured are abnormally red for a Scd spiral, see Paper I).

The emerging picture from the above considerations is that redder galaxies have redder central colors. The fact that the range of color indices at the outer regions is smaller than at the center would mean that the disks of different galaxies tend to be more alike than their bulges.

4.1.2. The properties of the bulges and disks

It is a well known fact that the output of the photometric decomposition of the light distribution in the image of a galaxy depends on the method used and on the form of the profiles adopted for the components (Knapen & van der Kruit 1991). To make explicit our choices we have used 1-D light profiles, with an exponential law for the disk (Freeman 1970) and the $r^{1/4}$ law for the bulge (de Vaucouleurs 1948), respectively:

$$\log(I_D^i) = \log(I_{D0}^i) - 0.7290(r/r_D^i - 1)$$

and

$$\log(I_B^i) = \log(I_{B0}^i) - 3.3307((r/r_B^i)^{1/4} - 1).$$

where i stands for the photometric band under consideration.

The isophotal profiles have been derived by plotting the isophotal levels *versus* their equivalent radii, calculated from the area inside each observed isophote. Disk and bulge parameters have been obtained from the surface brightness profiles, following Boroson (1981) and using the marking the disk method.

The main results are given in Table 1, and presented in the different panels of Figs. 2 and 3. (NGC 718 data appears as a discrepant point in all the relations involving its B-magnitude. We suspect that the abnormally red colors we have measured are not correct and the galaxy should be observed again before being included in the discussion. This is the reason to omit it in the following.) No trend is found between the disk and bulge parameters and the morphological type. In particular, for the Scs in our sample it is clear that their disk and bulge properties span a big range. Indeed, the size of our sample is too small to draw conclusions. But the trend we find for the isolated galaxies is much alike to that shown by larger samples of non-interacting galaxies. We have to insist, before starting comparisons between different sets of data, on the differences that can be induced by the use of different methodologies. Thus, it has been argued that exponential rather than $r^{1/4}$ fits would be more appropriate for the bulges of late spirals (Andreadakis & Sanders 1994; de Jong 1996a; Courteau, de Jong & Broeils 1996, Seigar & James 1998). The resulting bulges are then fainter than when a $r^{1/4}$ law is fitted. Moreover, the use of 1-D bulge profiles (our case) produce bulges with fainter central surface brightness and larger effective radii than 2-D fits.

With all this in mind, we can compare our results with the B-band data presented by de Jong (1996b) for a sample of non-perturbed, non-peculiar spiral galaxies, a sample that, as we already argued, can be taken as not too dissimilar to ours except in the luminosity range. In the same Fig. 2 we also present de Jong's data. It is clear that there is a large overlap between both sets of results.

The slight differences that can be appreciated after a more detailed look, can be explained in terms of the differences in methodology and the already quoted bias towards luminous galaxies in our sample. Thus, the mean value of the central disk surface brightness that we find is $\mu_B^0 = 20.9 \pm 0.6$, rather on the bright end of the values determined by Bosma & Freeman (1993) and by Giovanelli et al. (1994), and higher than the value given by de Jong. The same is found for the derived disk luminosities. This is certainly due to the absence of galaxies fainter than $M_B = -18$ in our sample since, as pointed out by de Jong (1996b) and Courteau (1996), the average value of the central surface brightness of the disks (Freeman 1970) depends on the luminosity range considered. Similar considerations apply to the bulge parameters we have derived.

We find that the scale length values for the disks depends on the photometric band (see Table 1), in the sense that it becomes

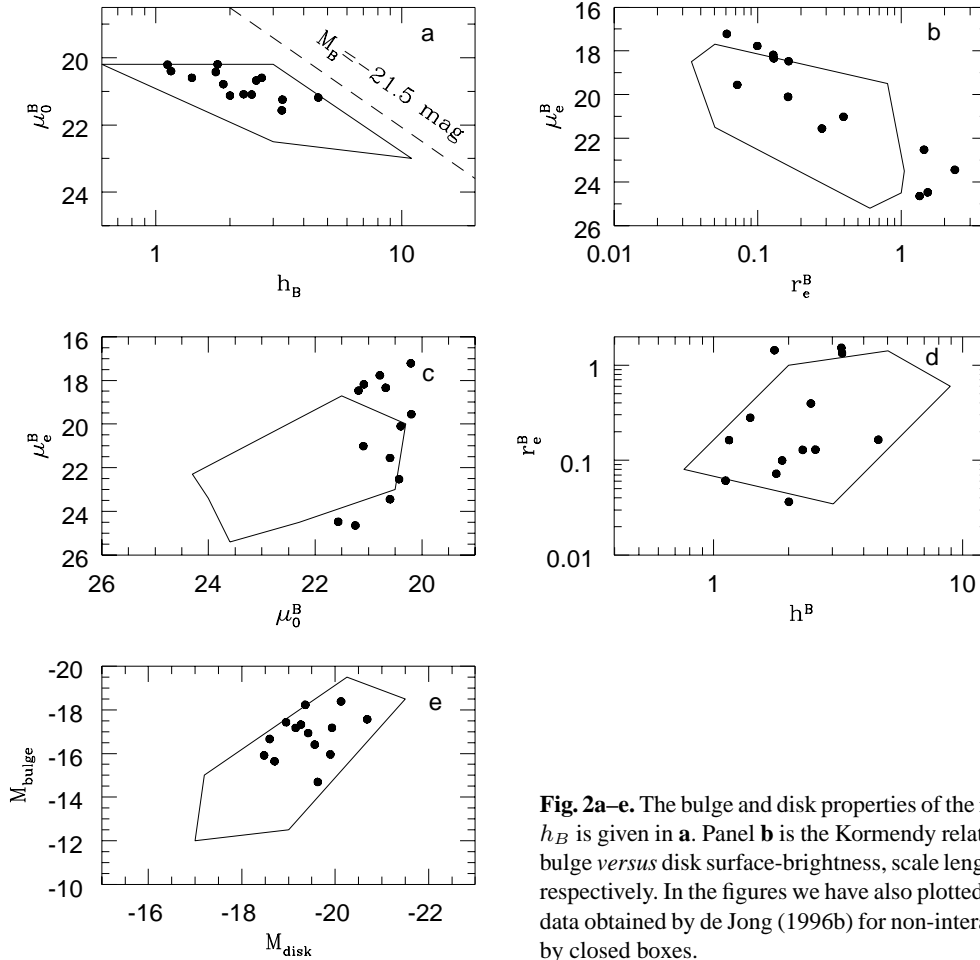


Fig. 2a–e. The bulge and disk properties of the isolated galaxies in the B band. μ_0^B versus h_B is given in **a**. Panel **b** is the Kormendy relation for the bulges of isolated spirals. The bulge versus disk surface-brightness, scale length and luminosity are shown in panel **c–e**, respectively. In the figures we have also plotted schematically the regions covered by the data obtained by de Jong (1996b) for non-interacting, non-perturbed spirals, represented by closed boxes.

smaller for redder wavelengths. Evans (1994) has argued that this would be due to the effect of dust layers in non-transparent disks, but de Jong (1996c), who found a similar result to ours, was able to model this behaviour by combining the presence of disk gradients in both, stellar age and metallicity.

On the other hand, the relations between the surface brightness and scale parameters for both components appear to be better correlated for our galaxies than for de Jong’s data (see panels a - disk - and b - bulge - of Fig. 2). The Kormendy relation for the bulge is significantly tighter for our data (in fact, de Jong reported no correlation between μ_e and r_e for his data). A similar relation appears for the disk, with a scatter much lower than previously found.

The relation between the corresponding parameters of the bulge and disk components are presented in the panels c, d and e in Fig. 2. It can also be seen that the range of values spanned by the disks is significantly smaller than that of the bulges. This would indicate that the spiral galaxies differ between them mainly by the bulge properties, the disks being much more similar.

We have also compared our results with the data presented by Baggett et al. (1998) in the V band (Fig. 3). The comparison indicates the same trends already noticed: The relations between parameters become tighter when only isolated or similar galax-

ies are considered. And, as before, the disk parameters span a significantly smaller range than the bulge parameters.

Thus, the trends shown by our data, in spite of the small sample we have, are supported as physically meaningful when larger samples of galaxies in acceptably similar conditions are considered. The data indicates that for isolated or non-interacting galaxies there is a tight relation between the surface brightness and size not only for the bulge (Kormendy relation) but also for the disk, and that these relations are more scattered when interacting galaxies are added. We will discuss in Paper II whether this is related to the lack of faint galaxies in our sample or to the interaction status. On the other hand, the disks of different spirals, no matter their morphological types, are much more alike than their bulges.

4.2. The kinematical properties. The masses and M/L ratios

The parameters describing the rotation curves are given in Table 10 of Paper I, whereas the median values are given in Table 1 here. We recall that the inner gradient, G (in $\text{km s}^{-1}\text{kpc}^{-1}$) is defined as $G = (v_G^{ob}/\sin(i))/r_G$, where r_G (in kpc) is the radius of the inner region of solid-body rotation, v_G^{ob} (in km s^{-1}) is the observed velocity amplitude at r_G , and i is the disk inclination, as derived from the optical images. Other parameters in

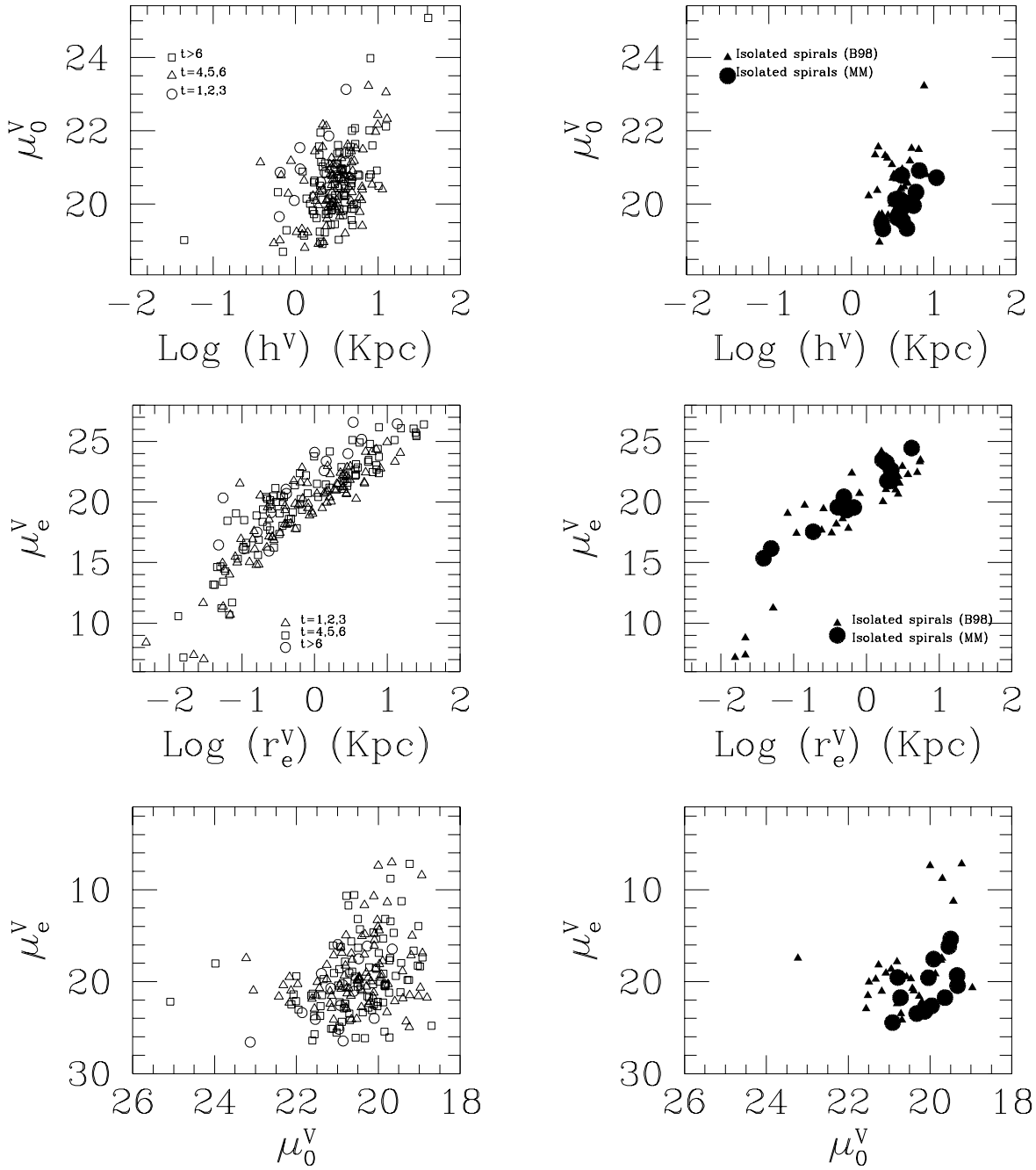


Fig. 3. Relations for bulge and disk parameters. In the *left panels* we plot data from all spirals with type I profiles from Baggett et al. (1998) (196 galaxies). Sa to Sb are plotted as open triangles, Sbc to Scd as open squares and later than Scd as open circles. In the *right panels* we only plot the galaxies selected from Baggett et al. as isolated (filled triangles), together with our sample spirals (dark circles).

the table are R_{max} (in kpc), the radius at the point of maximum rotation velocity, $V_{max}^i = V_{max}^{ob}/\sin(i)$; R_M , the radius at the last measured point in the rotation curve, with V_M its corresponding velocity. The mass has been evaluated at $0.5 \times D_{25}$, for a simple homogeneous and spherically symmetrical distribution, $M_{25} = 2.3265 \times 10^5 0.5 \times D_{25} V_{25}^2 M_\odot$ (Burstein & Rubin 1985).

Our results for V_M and M_{25} are in agreement with those found for Sb, Sbc and Sc galaxies by Rubin et al. (1982). With the mass calculated as described, we have evaluated the M/L

ratio for different bands. The median total mass-to-luminosity ratio is $M/L_B = 4.1 \pm 1.3$, spanning a range from 1.7 to 7.6. For the other bands we find similar ranges and central values, 5.5 ± 2.0 in V, and 4.5 ± 2.7 in I.

We choose the parameter $\Delta = tg^{-1}[(V_M - V_{max}) / (\max(V_M, V_{max})) \times (R_M - R_{max}) / (0.5 \times D_{25})]$ to describe the overall shape of the rotation curve farther than R_{max} . In other words, the velocities are normalised to the maximum amplitude and the radii to $0.5 \times D_{25}$. The parameter Δ can take

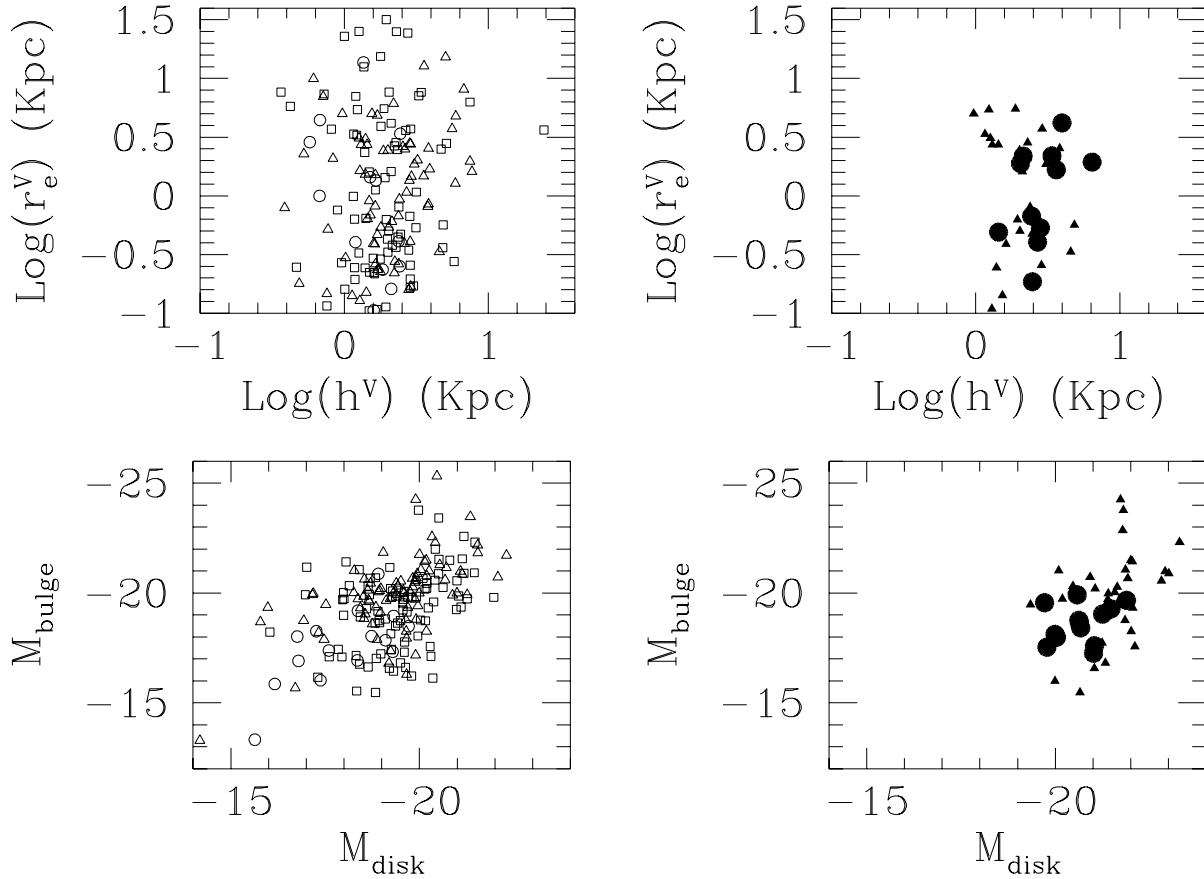


Fig. 3. (continued)

values around zero (for flat rotation curves), positive (for rising rotation curves), or negative (for declining rotation curves). The median value obtained for isolated galaxies, $\Delta \approx 8 \pm 7^\circ$, is compatible with flat rotation curves.

4.3. The star formation properties

A number of emission line regions, including all the nuclei we have observed, are present in our long slit spectra. Due to the wavelength coverage only the $[\text{OI}]\lambda 6300$, $\text{H}\alpha$, $[\text{NII}]\lambda\lambda 6548, 6583$ and $[\text{SII}]\lambda\lambda 6713, 6731$ lines could be detected. Our analysis will mainly concentrate on the properties of the strongest $\text{H}\alpha$ and $[\text{NII}]\lambda 6583$ lines.

The general aspect of all the spectra of the detected emission line regions, including the nuclei, is that of normal HII regions photoionized by stars. The $[\text{SII}]\lambda\lambda 6713, 6731$ line ratio is always ≥ 1 , indicating low electronic densities, as expected for such regions.

The median value of $\text{EW}(\text{H}\alpha)$ is 11 \AA and 18 \AA for the nuclei and the external regions, respectively. The $[\text{NII}]\lambda 6583/\text{H}\alpha$ line ratio ranges from 0.12 to 0.8 for all the nuclei with $\text{EW}(\text{H}\alpha) \geq 2 \text{ \AA}$, with a median value of 0.49. Indeed, for the 3 nuclei with $\text{EW}(\text{H}\alpha) < 2 \text{ \AA}$, the line ratio is very high, but this is due to the fact that the measure of the $\text{H}\alpha$ line intensity is severely affected by the underlying absorption.

For 104 of the 105 non-nuclear HII regions detected in our major axis long slit spectra the $[\text{NII}]\lambda 6583/\text{H}\alpha$ line ratio could be measured. The median value is 0.38, with 75% of the cases between 0.30 and 0.50. There are 4 extreme cases, with very high values, that are due to the presence of relatively strong absorption under $\text{H}\alpha$.

Thus the central values for nuclear and external HII regions are rather similar, with a larger range for the external regions. These results will be considered in more detail in Paper III, where they will be compared with data for HII regions in interacting galaxies.

Concerning the results from $\text{H}\alpha$ CCD photometry, we measured 7 isolated galaxies, whose total $\text{H}\alpha$ fluxes are given in Table 7 of Paper I (we have excluded NGC 718 from this analysis, since our spectroscopic data show that the contamination from $[\text{NII}]$ emission lines is very important, see Paper I). The median value for the total $\text{H}\alpha$ luminosity is $\log(\text{H}\alpha) = 7.89 \pm 0.55$ (in solar luminosities), that is well within the range found for spirals (Young et al. 1996, and references therein). The $\text{H}\alpha$ luminosities are well correlated with both the optical area of the galaxies and their FIR luminosities. From the first relation we derive $\text{H}\alpha \propto S$. This would mean that the average star formation per unit area, as judged from the $\text{H}\alpha$ luminosity is about the same in all isolated spiral galaxies.

The FIR luminosity was calculated as in Young et al., $L(FIR) = 3.75 \times 10^5 D^2 C [2.58S(60) + S(100)]$, where D is the distance to the galaxy in Mpc, C is a correction factor for the flux longwards of $120 \mu\text{m}$ and shortwards of $40 \mu\text{m}$ (they depend on $S(60)/S(100)$ and are taken from Table B.1 of the Catalogued Galaxies in the IRAS Survey, Lonsdale et al. 1985) and $S(60)$ and $S(100)$ are the IRAS 60 and $100 \mu\text{m}$ fluxes in Jy. In Fig. 4 we plot the comparison of $H\alpha$ and FIR luminosities for our sample galaxies, together with the points corresponding to the 10 galaxies catalogued as isolated by Young et al. Both samples of isolated spirals agree within the errors. They are all in the region occupied by normal spirals, compatible with ionization produced by O5 to B0 stars. We anticipate here that this is not the case for all the spiral in isolated pairs (Paper III).

Finally, we have also analysed the star formation history of those galaxies for which we have a complete set of data, i.e., the B-luminosity, the $H\alpha$ integrated flux, and the total mass. Following Gallagher et al. (1984), we quantify the present star formation rate in terms of the $H\alpha$ luminosity, the star formation rate during the past 10^9 years as a function of the B luminosity, and the initial star formation rate as a function of the total mass. Unfortunately we have all the relevant data for only 5 galaxies in our sample. Still, the result is compatible with a constant star formation rate along their lifetimes, with a smooth SFR, for the five galaxies. We will report in Paper III that this is not the case for some of the spiral galaxies in isolated pairs.

5. The relations between the measured parameters

It is well known that the observational parameters describing spiral galaxies are correlated, in such a way that two quantities can describe most of the variance in the parameter space. In his pioneering analysis, Brosche (1973) used the method of the Principal Component Analysis (PCA) to study the data (morphological type, optical size, color, absolute luminosity, maximum rotation velocity and HI mass) of 31 spiral galaxies. He found that the parameter space has two significant dimensions. Bujarrabal et al. (1981) also used the PCA to study a sample of ≈ 100 objects with optical and radio data and also conclude that 2 parameters could suffice to describe the data: *size* (given equivalently by the optical size, the HI mass or the luminosity) and *aspect* (given by the morphological type or the color). Whitmore (1984) obtained the same conclusion for a sample of 60 spirals with about 30 observed parameters, and assigned the two dimensions to *scale* (optical size, luminosity) and *form* (color, bulge to total light ratio). More recently, the PCA of I-images of some 1600 spirals led Han (1995) to find also two principal dimensions. Magri (1995), with a sample of 492 spirals with compiled and new data (Magri 1994), and a refined version of the PCA to allow for the inclusion of non-detections, also concluded in the same vein.

Even if the PCA has some limitations related with the bias in the results that could be introduced if the number of parameters involved in the analysis is not big enough (Magri 1995), or the fact that it assumes that the correlations among the parameters are strictly linear, it appears as a well suited method

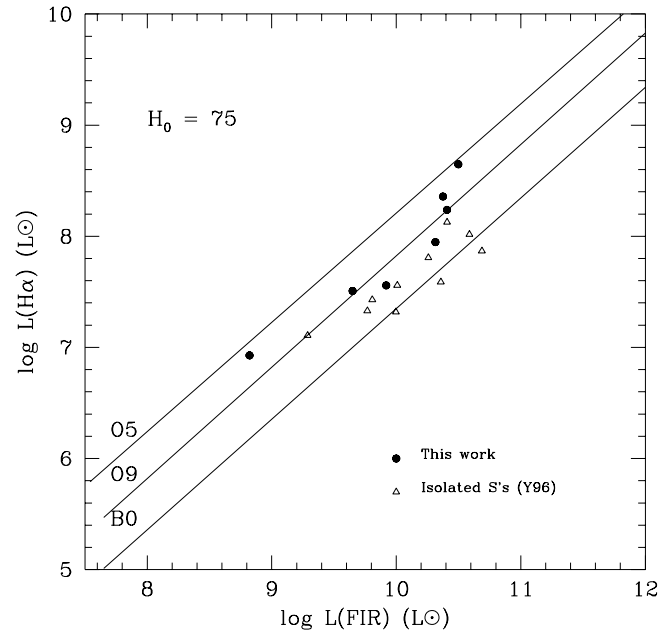


Fig. 4. Relationship between integrated $H\alpha$ and FIR luminosities. Solid dots are for our isolated spiral galaxies, triangles are for the sample of isolated galaxies by Young et al. (1996). The solid lines represent the expected relations for O5, O9 and B0 stars, as presented by Devereux & Young (1990)

to find the minimum number of variables describing the data set we have constructed for isolated spiral galaxies. In our case, given that all possible effects of the interaction are in principle excluded, what could be expected from that kind of analysis is to obtain the bare, intrinsic structural correlations between the parameters. We have already discussed how the inclusion of interacting galaxies could increase the scatter in the relations between parameters. In the same sense, Folkes et al. (1996) have shown that the inclusion of perturbed or peculiar galaxies could produce misleading results, in the sense of smoothing the morphology-spectrum relationship found for normal galaxies.

The main result that emerges from the PCA of our data is that the parameter space has essentially 2 dimensions, in agreement with all the previous results. The new aspects of our analysis are that till 95 % of the variance of the sample is explained, and the identification of a better suited form parameter. Indeed, the first *eigenvector*, corresponding to the *scale* parameter, is given by either the total luminosity, L_B , the total mass, M , or the size, as usual. For the second, the *form* parameter, we find that the best choice is the inner gradient, G , or, equivalently, the bulge to disk ratio, B/D . In Fig. 5 we show the projection of the vector constructed with the luminosity, the bulge to disk ratio, the total mass, the G parameter and a color index onto the plane described by the two eigenvectors. We note that we find no correlation between the color and the luminosity, whereas color is correlated with the bulge-to-disk ratio, in the expected sense of redder galaxies having a greater relative contribution from the bulge component.

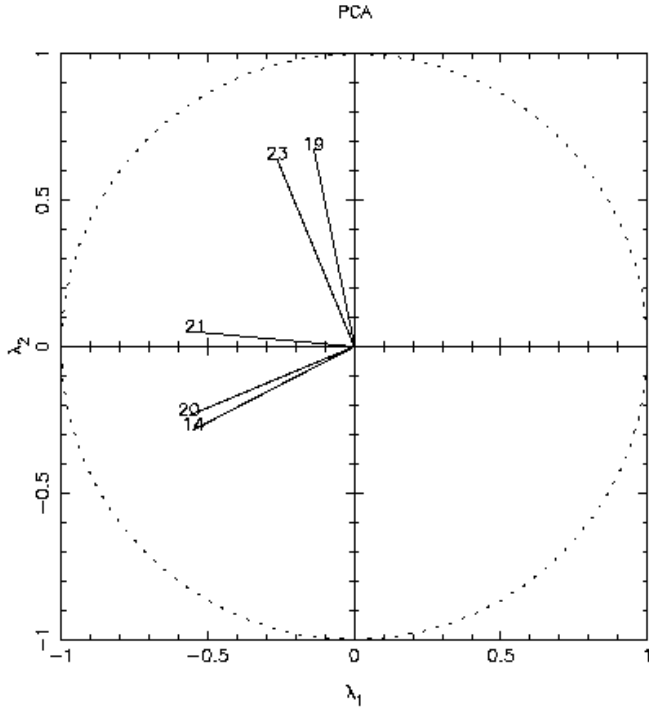


Fig. 5. Results of the PCA. The vectors are 14=G, 19= L_B , 20= B/D=, 21=(B-V), 23=Mass.

It is the first time that the G-parameter is revealed as equivalent to the form *eigenvector*. Some other were proposed, like some color index, or the morphological type, but what our data on isolated galaxies show is that the scatter is minimum when G, or the B/D ratio, is used. The general trends between the morphology, the colors and the B/D ratios are well known, and at the base of the Hubble classification scheme. In that sense, Whitmore (1984) pointed out that the inner gradient of the rotation curves could be a good discriminant of the central density, i.e., the importance of the bulge component. On the other hand, Baiesi-Pillastrini (1987) already noticed that the G-parameter is not directly correlated with the morphological type, so the relation between the B/D ratio and the morphology would present an important scatter, as it is. What we find here is that the G-parameter is a much more useful property to classify a spiral galaxy, in the sense that it is essentially coincident with one of the 2 *eigenvectors* of the parameter space, i.e., normal to the size parameter (see Fig. 5).

Indeed, a number of strong linear correlations between parameters does exist. Regarding the photometric data, we have already pointed out that the optical size and the luminosity in each band are well correlated. The disk and bulge parameters, that have been discussed in the previous section, also present good correlation, the tightest being between the surface brightness and the size, both for the bulge (the Kormendy relation), and for the disk. For the bulge parameters, we find $I_e \approx r_e^{0.64}$, i.e., somewhat smaller slope but compatible with that of the Kormendy relation for other spiral bulges (Andredakis et al. 1995; Hunt et al. 1998) and for ellipticals (Bender et al. 1992).

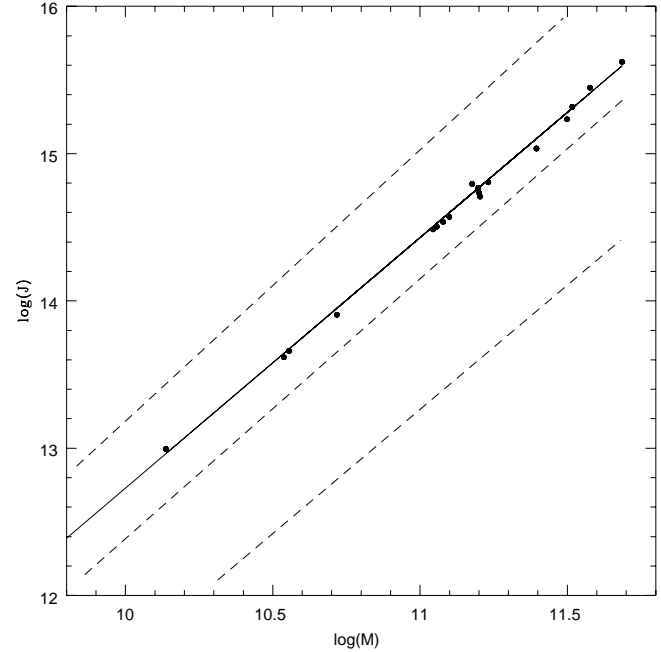


Fig. 6. Correlation between the angular momentum, J (see text) and the total mass, M . The dashed lines represent the average and range found in Campos-Aguilar et al. (1993). The solid line corresponds to the fit to our data, $\log(J) = -4.27 + 1.70 \times \log(M)$.

Among the relations involving kinematical parameters, we find a correlation between V_M and the size, in agreement with the linear relationship found by Zasov & Osipova (1987). V_M (and V_{max}) are also related with the B luminosity (Rubin et al. 1982; Persic & Salucci 1991). We also find a good correlation between the angular momentum, $J = M \times V \times R$, and the total mass, $\log(J) = -4.27 (\pm 0.24) + 1.70 (\pm 0.02) \times \log(M)$, in good agreement with Campos-Aguilar et al. (1993). The scatter is smaller in our case (see Fig. 6). V_{max} and R_{max} are correlated with the total magnitude with the same overall tendencies found by Courteau & Rix (1997) (they use R magnitudes from Courteau 1996) but, at variance with them, we do not find any clear trend between total colors and total luminosity, what could be due to the limited luminosity and subtype range covered by our sample. Total absolute luminosity and total mass are well correlated, as shown in Fig. 7. We obtain $M = 4.80 (\pm 0.15) \times L_B$ with a correlation coefficient $r = 0.9$. This implies a mass to luminosity ratio which is within the range of (M/L) values (from 3.9 to 6.6 in solar units, with $H_0 = 75 \text{ km s}^{-1} \text{ Mpc}^{-1}$) measured for Sc galaxies by Rubin et al. (1985). It is also compatible with (M/L_R) ratios found for field galaxies by Forbes (1992) (from 3 to 6 in solar units, with $H_0 = 75 \text{ km s}^{-1} \text{ Mpc}^{-1}$). M/L ratio tends to be higher for more massive (or more luminous) galaxies, as found by Broeils & Courteau (1996).

The new result is the tight correlation between the inner gradient, G, and the bulge to disk ratio, B/D (Fig. 8) we have found. The slope is $(6.80 \pm 0.16) \times 10^{-4}$ and the scatter amounts only to 0.02 in the determination of B/D. As already mentioned, either of those two parameters builds up the second *eigenvector* of the parameter space of the isolated spiral galaxies. The exist-

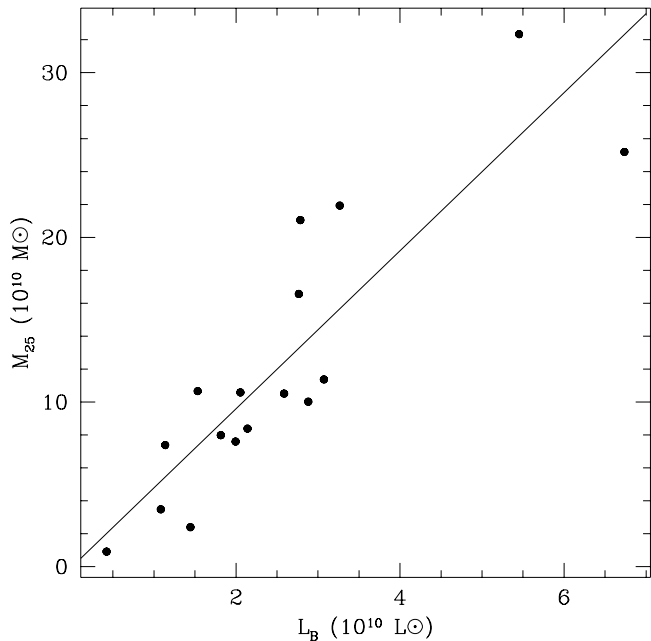


Fig. 7. Correlation between the mass inside $0.5 \times D_{25}$, M_{25} (see text) and the total luminosity in B, L_B .

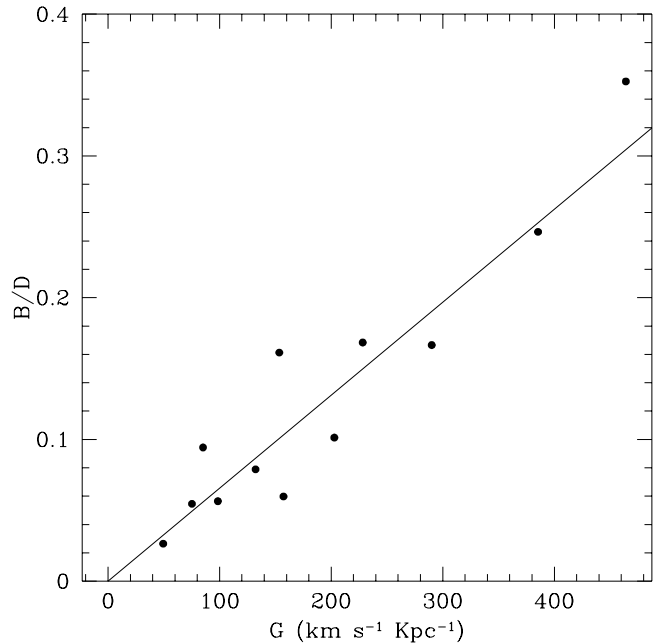


Fig. 8. Correlation between the inner gradient of the rotation curve, G ($\text{km s}^{-1} \text{Kpc}^{-1}$), and the bulge to disk luminosity ratio, B/D .

ing correlation reflects what could be intuitively expected, that is, that galaxies with bigger bulges have higher inner gradients. Baiesi-Pillastrini (1988) found a somewhat similar correlation but much more scattered. This could be due to the inclusion of non-isolated spirals in his sample since, as we show in the next Paper III of the series, the correlation is affected by the interaction, as it is much weaker for spirals in pairs.

The correlation between G and the B/D ratio can in principle be used for distance determination. We notice however that, as just mentioned, the scatter of the relation increases when non isolated galaxies are considered, so only strictly isolated galaxies should be used.

6. Conclusions

We have characterized a sample of spirals selected as being isolated, in order to use it for comparisons with the analogous properties of spirals in different environmental situations. We caution that we have selected bright galaxies (brighter than $M_B = -18.5$) and that the sample is too small to attempt the analysis by morphological types. We further notice that the sample is dominated by Sc type galaxies. Whether this is due to the small size of the sample or it reflects the nature of isolated spiral galaxies should be further analyzed with larger samples. We point out that similar results are obtained when existing larger samples of non-perturbed galaxies are examined, so the possibility that there is a preference for later types in poor environments should be explored.

We have used total parameters, as luminosity, color indices and mass, together with others describing their photometrical or kinematical behaviour in more detail, as the bulge/disk ratio, the

color gradients or the shape of the rotation curve. The isolated spirals we have analyzed can be described as following:

- The overall morphological aspect is quite symmetric and regular, as expected for galaxies supposed to be free of external influences in the last 10^9 years at least. On the other hand, the fraction of barred galaxies is similar to what is found for spirals irrespective of their environmental situation. Moreover, all of them show the presence of features indicative of non-axisymmetric components of the gravitational potential. Therefore, one is led to conclude that either the life time of these features is significantly over 10^9 years or that they can be spontaneously formed along the life of a galaxy.
- The total and central color indices are well correlated: redder galaxies have also redder central regions. The outer parts of the disks are bluer and more similar than the central parts.
- All of the galaxies in our sample without exception show Type I photometrical profiles. As we will show in Paper III, this is not the case for non-isolated spirals, that can present Type II profiles. The range of the disk scale lengths and effective surface brightness seems to be narrower for isolated spirals than for samples including galaxies in other situations. The disks of different isolated galaxies are bluer than their central regions, and much more alike that the bulges.
- Their current star formation rates as given by total $H\alpha$ (or FIR) luminosities are within the range found for spirals classified as normal, i.e., without apparent peculiarities in their morphology or nucleus. The line ratios measured in the observed emission line regions indicate that they are photoionized by stars. For the cases for which the history of the star

formation could be retraced, it is found compatible with a smooth, constant SFR along their lifetimes.

- The overall shape of their rotation curves from R_{max} to R_M can be described as flat. The median value of the slope in that region is found to be $8 \pm 7^\circ$.
- We have applied the PCA to the data set we have constructed. In agreement with previous studies on larger samples including non isolated galaxies, we find that the isolated spirals in our sample constitute a family that can be described by two main dimensions given by size (either the luminosity, the optical size or the total mass) and form (either the inner gradient of the rotation curve, the G-parameter, or the bulge-to-disk luminosity ratio, B/D). The remaining variance could just be due to the errors in the parameters. We conclude that G or B/D are more robust and objective parameters than the morphological subtype or the color indices for the classification of spiral galaxies.
- Previous bi-variate relations are confirmed, as those between the mass and the luminosity, the size or the angular momentum.
- We have found for the first time a very tight correlation between G and B/D. B/D is a distance independent parameter, whereas G is not. We point out that the correlation G-B/D, constitutes a new distance indicator. We stress however that it would only be well suited for isolated systems since, as illustrated in Paper III, the scatter of the relation significantly increases when interacting galaxies are included.
- The isolated spiral galaxies define very tight structural relations. The bulges define the Kormendy relation with a small scatter. A similar relation is found for the disks, with a lower scatter than in previous studies. The scatter in those relations, or in the G-B/D relation, increases significantly when interacting galaxies are included. Whether this is related to the inclusion of fainter galaxies or to the interaction status will be discussed in Paper III.

Acknowledgements. We acknowledge financial support by the Spanish DGICYT, under the program PB93-0139. One of us, IM, acknowledges a grant from the Spanish Ministerio de Educación y Ciencia, EX94 08826734, and the hospitality of the Institut d'Astrophysique de Paris, where the writing of this paper was started. The Isaac Newton and Jacobus Kaptejn Telescopes are operated on the island of La Palma by the Royal Greenwich Observatory in the Spanish Observatorio del Roque de los Muchachos of the Instituto de Astrofísica de Canarias. This research has made use of the NASA/IPAC EXTRAGALACTIC DATABASE (NED) which is operated by the Jet Propulsion Laboratory, Caltech, under contract with the National Aeronautics and Space Administration.

References

- Andredakis Y.C., Sanders R.H., 1994, MNRAS 267, 283
 Andredakis Y.C., Peletier R.F., Balcells M. 1995, MNRAS 275, 874
 Arsenault R., 1989, A&A 217, 66
 Athanassoula E., 1984, Physics Reports 114, 319
 Baesi-Pillastrini G.C., 1987, A&A 1972, 375
 Baesi-Pillastrini G.C., 1988, Astron. Lett. Comm. 27, 27
 Baggett W.E., Baggett S.M., Anderson K.S.J., 1998, AJ 116, 1626
 Bender R., Burstein D., Faber S.M., 1992, ApJ 399, 462
 Boroson T., 1981, ApJS 46, 177
 Bosma A., Freeman K.C., 1993, AJ 106, 1394
 Broeils A.H., Courteau S., 1996, astro-ph/9610264
 Brosche P., 1973, A&A 23, 259
 Bujarrabal V., Guibert J., Balkowski C., 1981, A&A 104, 1
 Burstein D., Rubin V.C., 1985, ApJ 297, 423
 Byrd G.G., Howard S., 1992, AJ 103, 1089
 Campos-Aguilar A., Prieto M., García C., 1993, A&A 276, 16
 Combes F., Elmegreen B.G., 1993, A&A 271, 391
 Courteau S., 1996, ApJS 103, 363
 Courteau S., de Jong R.S., Broeils A.H., 1996, ApJ 457, L73
 Courteau S., Rix H.W., 1997, ApJL submitted
 de Jong R.S., van der Kruit C., 1994, A&AS 106, 451 (dJ1)
 de Jong R.S., 1996a, A&AS 118, 537 (dJII)
 de Jong R.S., 1996b, A&A 313 45 (dJIII)
 de Jong R.S., 1996c, A&A 313,377 (dJIV)
 de Vaucouleurs G., 1948, Ann. Astrophys. 11, 247
 de Vaucouleurs G., de Vaucouleurs A., Corwin H.G., 1976, Second Catalogue of Bright Galaxies. University of Texas Press, Austin, USA (RC2)
 de Vaucouleurs G., de Vaucouleurs A., Corwin H.G., et al., 1991, Third Reference Catalogue of Bright Galaxies. Springer, New York (RC3)
 Devereux N., Young J.S., 1990, ApJL 350, L25
 Elmegreen D.M., Elmegreen B.G., Bellin A.D., 1990, ApJ 364, 415
 Evans R., 1994, MNRAS 266, 511
 Folkes S.R., Lahav O., Maddox S.J., 1996, MNRAS 283, 651
 Forbes D.A., 1992, A&AS 92, 583
 Freeman K.C., 1970, ApJ 160, 811
 Gallagher J.S., Hunter D.A., Tutukov A.V., 1984, ApJ 284, 544
 Giovanelli R., Haynes M.P., Salzer J.J., Wegner G., da Costa L.N., 1994, AJ 107, 2036
 Han M., 1995, ApJ 442, 504
 Héreaudeau Ph., Simien F., 1996, A&AS 118, 111
 Huchra J., Davis M., Latham D., Tonry J., 1983, ApJS 52, 89
 Hunt L.K., Malkan M.A., Moriondo G., Salvati M., 1998, astro-ph/9808168
 Karachentsev I.D., 1972, Soob. Sb. Asrt. Observatory Akad. Nauk, 7
 Kent S.M., 1988, AJ 96, 514
 Knapen J.H., van der Kruit P.C., 1991, A&A 248, 57
 Lonsdale C.J., Helou G., Good J.C., Rice W., 1985, Catalogued Galaxies and Quasars Observed in the IRAS Survey, JPL Publ. No. D-1392
 Magri C., 1994, AJ 108, 896
 Magri C., 1995, AJ 110, 1614
 Márquez I., Moles M., 1996, A&AS 120, 1 (Paper I)
 Márquez I., Moles M., Masegosa J., 1996, A&A 310, 401
 Mathewson D.S., Ford V.L., Buchhorn M., 1992, ApJS 81, 413
 Moles M., Márquez I., Pérez E., 1995, ApJ 438, 604
 Moles M., Márquez I., Masegosa J., et al., 1994, ApJ 432, 135
 Peletier R.F., Balcells M., 1997, New Astronomy 1, 349
 Persic M., Salucci P., 1991, ApJ 368, 60
 Pierce M.J., Tully R.B., 1992, ApJ 387, 47
 Roberts M.S., Haynes M.P., 1994, ARA&A 32, 115
 Rubin V.C., Ford W.K., Thonnard N., Burstein D., 1982, ApJ 261, 439
 Rubin V.C., Burstein D., Ford W.K., Thonnard N., 1985, ApJ 289, 81
 Rubin V.C., Hunter D., Ford W.K., 1991, ApJS 76, 153
 Seigar M.S., James P.A. 1998, MNRAS (submitted, astro-ph/9803253)
 Simkin S.M., Su H.J., Schwarz M.P., 1980, ApJ 237, 404

Soares D.S.L., 1989, Ph.D. Thesis, University of Groningen, NL

Sundelius B., Thomasson M., Valtonen M.J., Byrd G.G., 1987, A&A
174, 67

Turner E.L., 1976, ApJ 208, 20

Whitmore B.C., 1984, ApJ 278, 61

Young J.S., Allen L., Kenney J.D.P., Lesser A., Rownd B., 1996, AJ
112, 1903 (Y96)

Zasov A.V., Osipova T.A., 1987, Sov. Astron. Lett. 13, 7020